Simulation of clustering and anisotropy due to Co step-edge segregation in vapor-deposited $CoPt_3$

B. B. Maranville,* M. Schuerman, and F. Hellman†
Physics Department, University of California at San Diego, San Diego, California 92093, USA
(Received 21 July 2005; revised manuscript received 20 January 2006; published 22 March 2006)

An atomistic mechanism is proposed for the creation of structural anisotropy and consequent large perpendicular magnetic anisotropy in vapor-deposited films of $CoPt_3$. Energetic considerations of bonding in Co-Pt suggest that Co segregates to step edges due to their low coordination, for all film orientations, while Pt segregates to the two low index surfaces. Coalescence of islands during growth cause these Co-rich step edges to become flat thin Co platelets in a Pt rich matrix, giving rise to the experimentally observed magnetic anisotropy. This proposed model is tested with kinetic Monte Carlo simulation of the vapor deposition growth. A tight-binding, second-moment approximation to the interatomic potential is used to calculate the probability of an atom hopping from one surface site to another, assuming an Arrhenius-like activation model of surface motion. Growth is simulated by allowing many hopping events per adatom. The simulated as-grown films show an asymmetry in Co-Co bonding between the in-plane and out-of-plane directions, in good agreement with experimental data. The growth temperature dependence found in the simulations is strong and similar to that seen in experiments, and an increase in Co edge segregation with increasing temperature is also observed.

DOI: 10.1103/PhysRevB.73.104435 PACS number(s): 75.70.−i, 75.30.Gw, 81.15.Aa, 81.10.Aj

I. INTRODUCTION

It has been known for some time that films of $CoPt_3$, codeposited within a specific temperature range, possess a strong perpendicular magnetic anisotropy.[1–5] The anisotropy far exceeds the possible contribution from bulk magnetoelastic strain, and a nanoscale structural anisotropy is believed to be responsible for the effect; small platelets of Co are formed on the growth surface and are preserved, once buried by later adatoms, due to the low bulk mobility below approximately $\frac{1}{3}T_{\text{melting}}$.[5] The existence of enhanced in-plane Co clustering has been verified with extended x-ray absorption fine structure (EXAFS) studies,[6–8] despite the negative energy of mixing of Co and Pt in the bulk. Co-Pt and Co-Pd alloys with perpendicular magnetic anisotropy may be useful to the magnetic recording industry for perpendicular or patterned media. Control and understanding of the length scale of the Co clustering which leads to the magnetic anisotropy is essential to their use, particularly as the bit size continues to decrease.

An atomistic model of how and why this Co clustering occurs has not been developed up to this point. Models proposed to date for the source of the anisotropy either suggest an incomplete surface segregation whose details are unclear,[5] or rely only on (111) growth mechanisms,[7] while data show that the anisotropy is found also in (100)- and (110)-oriented films.[5]

In this paper we explore the energetics at the surface, using realistic interatomic interaction potentials. We determine that Co is likely to segregate to step edges on the growing surface, and show that this leads to in-plane clustering in the resulting complete layers. We perform a kinetic Monte Carlo simulation of the growth using calculated hopping probabilities, the results of which show a connection between edge segregation and Co clustering. In particular, an increase in both Co edge segregation and chemical anisotropy is seen as the simulation temperature is increased, in agreement with previous experimental data.

It has been shown, experimentally and theoretically, that Pt will preferentially segregate to the surface of a (111)-or (100)-oriented Co-Pt alloy film, while Co will segregate to the surface of a (110)-oriented film.[9–11] The Pt coverage on the (111) surface is found to be close to 100% in a dilute film of $Co_{20}Pt_{80}$, but even more remarkable is the complete coverage of a single monolayer of Co deposited on Pt, by Pt from the subsurface. By contrast in (110) films, an almost pure Co surface layer is found. Pt segregates to the nine- and eight-fold coordinated surface sites of the (111) and (100) surfaces, while Co segregates to the sevenfold coordinated surface sites of the (110) surface. It is therefore clear that the surface energy of Pt at higher coordination numbers is less than that of Co, but reverses at lower coordination. The surface energy can be thought of as the difference between the binding energy of an atom in the bulk and one on the surface, thus the last four (out of 12) bonds of Pt are weaker than in Co. The bulk binding energy[12] of Pt (5.853 eV/atom) is considerably higher than that of Co (4.39 eV/atom), however, and therefore at low coordination numbers Pt bonds are stronger than equivalent Co bonds. We are provided with a convenient breakpoint: As the sevenfold coordinated (110) surface shows Co segregation, the point at which the energy per Pt bond exceeds the energy of a Co bond must lie between a coordination number of seven and eight [the (100) surface].

We carry out a calculation using the tight-binding second-moment approximation to the interatomic potential, which agrees with these qualitative arguments. A surface segregation of Pt in the (111) and (100) surface is seen in the calculation, with a crossover to Co segregation below a coordination number of seven. These calculations show that Co should segregate to step edges, due to these sites' low coordination. A kinetic Monte Carlo simulation of epitaxial growth, based on these potentials, shows Co edge segregation and the resulting creation of preferential in-plane Co-Co

pairs during growth. Since epitaxial $CoPt_3$ [both (100) and (111)] has been shown to grow via three-dimensional (3D) island growth,[13] small Co platelets form from the intersection of step edges. These platelets cause the observed perpendicular magnetic anisotropy, much as is found in Co/Pt multilayers.

II. INTERATOMIC POTENTIALS AND SURFACE EQUILIBRIUM

We have used the tight-binding, second-moment approximation (TB-SMA) to the interaction potential for atoms on the surface of the growing film. This potential has been shown to be highly accurate in modeling of both *d*-band and noble metals, so it is ideal for the study of Co and Pt.[14] Equations (1) and (2) show the two components of this potential, one repulsive (E_R) and one attractive (E_B); both potentials decay exponentially with the distance between the atoms, and $E_{\text{total}}=E_R+E_B$.

$$E_R = \sum_j A_{\alpha\beta} e^{-p_{\alpha\beta}\left(r_j/r_0^{\alpha\beta}-1\right)}, \tag{1}$$

$$E_B = -\left[\sum_j \xi_{\alpha\beta}^2 e^{-2q_{\alpha\beta}\left(r_j/r_0^{\alpha\beta}-1\right)}\right]^{1/2}. \tag{2}$$

The repulsive part has an energy prefactor A (in electron volts) and an exponential decay constant p. Similarly, the bonding part has an energy prefactor of ξ and a decay constant q. The equilibrium interatomic spacing is represented by r_0, and the subscripts α,β represent the species involved (here, Co and Pt). The repulsive core component is a linear combination of surrounding atoms, representing the ion-ion repulsion of the atom cores. The bonding component, however, scales as the square root of the number of neighbors. This is because in metallic bonding, the bonding energy is dependent on the width of the electron density of states (DOS), which varies as the square root of the second moment μ of the DOS, with μ varying linearly with coordination number. Thus $E_B \propto \sqrt{\mu} \propto \sqrt{z}$, where z is the coordination number.[14] This nonlinear dependence of the binding energy on the coordination number greatly influences calculations of surface energies, in that each successively added bond has reduced value compared with the first bond.

The values of $A_{\alpha\beta}$, $\xi_{\alpha\beta}$, $p_{\alpha\beta}$, and $q_{\alpha\beta}$ for $\alpha=\beta=\{\text{Co or Pt}\}$ are taken from the literature[14] for Co-Co interactions and Pt-Pt interactions, in which the potential was fit to the cohesive energy of the solid, the equilibrium lattice constant and the elastic constants.[15] These values are listed as the first two rows in Table I. The values for the Co-Pt interaction, $\alpha=$Co and $\beta=$Pt, were then determined, by setting lengths $p_{\alpha\beta}$, $q_{\alpha\beta}$, and r_0 for the Co-Pt bond to the arithmetic average of the corresponding lengths for Co and Pt. The energy of a simulated lattice of $CoPt_3$ was then calculated. By requiring that $dE/dr_0=0$ for r_0 equal to the measured lattice constant of $CoPt_3$, and that the total energy of the system equals the weighted average of the cohesive energies of Co and Pt plus the experimentally measured energy of mixing, we solved for ξ and A. The energy of mixing, $E_{\text{mix}}=-0.26$ eV per Co atom, was taken from the literature for a dilute mixture of Co in Pt,[16] with the negative sign indicating that mixing is energetically favored. The resulting values of A, ξ, p, and q for the Co-Pt interaction are presented in the last row of Table I.

TABLE I. Parameters of tight-binding potentials.

	Parameters			
α,β	$A_{\alpha,\beta}$(eV)	$\xi_{\alpha,\beta}$(eV)	$p_{\alpha,\beta}$	$q_{\alpha,\beta}$
Co, Co[a]	0.0950	1.4880	11.604	2.286
Pt, Pt[a]	0.2975	2.6950	10.612	4.004
Co, Pt[b]	0.3472	4.0367	11.108	3.145

[a]From Reference 14.
[b]Calculated as described in the text.

Using these parameters, we find that the completely $L1_2$-ordered bulk phase of $CoPt_3$ is energetically favored over a random or clustered film, consistent with the known phase diagram of Co-Pt bulk alloys.[17] On the surface, however, the lowered coordination number leads to a different lowest-energy state, also as experimentally observed. The total cohesive energy of Pt, $E_c(\text{Pt})=5.853$ eV is greater than $E_c(\text{Co})=4.40$ eV,[12] therefore in a linear bond-counting model one might expect Co would always segregate to the surface of a Co-Pt alloy, thereby minimizing the energy of the broken bonds. It is however experimentally known that Pt segregates to the surface of a Co-Pt alloy film, therefore the surface free energy of Pt is lower than that of Co.

The nonlinear TB-SMA potential correctly describes this behavior, showing that the energy per added nearest neighbor of Co exceeds that of Pt for a higher coordination number, so that the surface free energy of Co is higher than Pt, consistent with other theoretical models for Co-Pt.[18] Using a simplified calculation of surface energies assuming no relaxation and nearest neighbors only, we calculate the binding energy for atoms versus the number of nearest neighbors (NN) in pure Co and Pt. The results of this calculation are plotted in Fig. 1. Here the binding energy is defined as the total bond energy for an atom relative to the free state with zero NN, which would have zero binding energy, while atoms with 12 NN have the full cohesive energy of the respective solid material (4.40 eV for Co, 5.853 eV for Pt). Accordingly, in a simple linear bond-counting model the energies would be straight lines on this plot, with the binding energy for Co always lower than for Pt. In the TB-SMA, the total integrated energy remains higher for Pt, due to the much higher energy per neighbor at lower coordination number, yet the energy per added bond of Co above nine nearest neighbors (NN) is significantly higher. The shape of this curve yields a critical coordination number between six and seven, below which Co is favored to migrate to lower-coordinated sites, and above which Pt migrates to lower-coordinated sites. Using this critical number, we predict that Pt will segregate to the (111) and (100) surfaces (9 and 8 NN, respectively) but this tendency will disappear for the sevenfold coordinated surface sites of (110)-terminated Co-Pt alloys, all in agreement with experimental observations.[9–11]

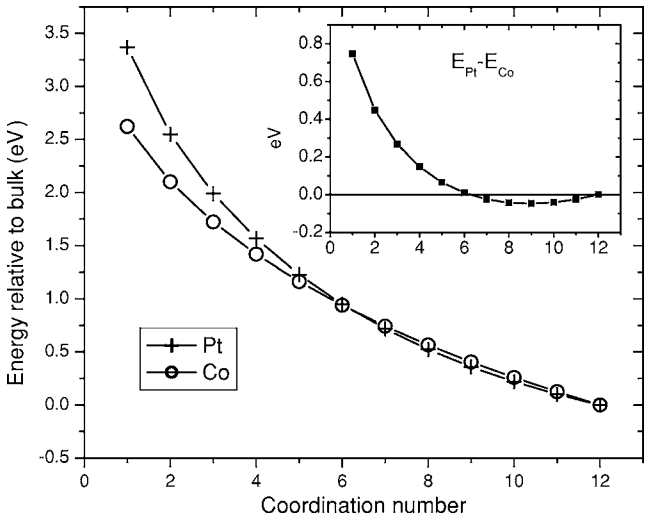

FIG. 1. Binding energy added for each additional neighbor, assuming pure Co environment for Co and pure Pt environment for Pt. Inset shows difference between Co and Pt binding energy versus coordination number. Note sign change between six and seven.

Based on this observation, we predict that Co atoms on the surface will preferentially segregate to the edges of growing steps. On a (111)-oriented surface, an atom completely embedded in an island has nine NN, while an edge atom has seven, and corner atoms have six or five NN. On a (100) surface an embedded atom has eight NN, an edge atom has six NN, and a corner atom has five NN. On a (110) surface, the embedded atoms have only seven NN, close to the boundary between Co and Pt segregation, so less edge segregation is predicted. The predicted segregation will tend to concentrate Co at step edges, which we suggest is the root cause of planar clustering and consequent magnetic anisotropy in $CoPt_3$ films. In previous studies of Co growth on vicinal Pt, clusters of Co were seen to grow in a certain temperature range with very little mixing of Co and Pt at step edges.[19] This contrasts with a Ni on Pt study in which edge segregation of Ni is observed concurrent with the formation of an ordered edge state of alternating Ni and Pt.[20]

III. GROWTH SIMULATION

The binding-energy calculation results are used in a kinetic Monte Carlo simulation of the surface dynamics of this alloy. We assume a solid-on-solid model in which atoms are only allowed to occupy (or hop to) a site if all the nearest-neighbor sites immediately below are occupied. An atom is not permitted to hop if any atoms rest on top of it. Neither interlayer transport nor movement of buried atoms is permitted in the model. This limit of no interlayer exchange is appropriate as the effect we are interested in (formation of Co clusters leading to magnetic anisotropy) occurs in a growth temperature regime where surface mobility is high but bulk mobility is experimentally known to be negligible.[4,5] This approach has been used previously to model many other growth systems, such as Pt on Pt growth.[21] The substrate or zeroth layer on which the simulation atoms are placed is a layer composed of a random arrangement of one Co atom for each three Pt atoms, and the lattice is constrained to have the same spacing as a $CoPt_3$ film. For all our simulations, a (100)-oriented crystal lattice is assumed for simplicity.

Surface dynamics are simulated by allowing atoms to diffuse. Hopping rates for atoms on the surface of the material are calculated using a thermally activated probability for hopping, with a rate $R_{\mathrm{hop}}=R_0 e^{-E_b/kT}$ exponentially dependent on the energy barrier E_b with a prefactor (attempt frequency) R_0 of 10^{11} s^{-1}. This prefactor is at the low end of a range of observed surface-diffusion barriers.[22–24] Every rate scales linearly with R_0, so the exact choice affects only the time scales in the problem and not the relative probabilities of one hopping event versus another. Thus, in the growth simulations the only effect of increasing the prefactor by a factor of 10 would be to reduce the effective deposition rate by a factor of 10.

The barrier energy E_b is calculated using the interatomic potentials described in the previous section, taking into account only nearest neighbors. All possible hopping events are tabulated, with the following constraints: Any surface atom with less than four in-plane NN is considered a possible starting point, and any unoccupied NN site is a possible end point for a hop. The lowest-energy spatial pathway between the start and end points of a hop, and the highest potential along that path, are determined using the nudged elastic-band method first described by Ulitsky and Elber.[25] Even with only nearest-neighbor interactions considered, this leads to 93 312 different possible hop energies.

The average values of the hopping energy of a Pt atom on a clean Pt surface, can be compared to previous calculations and measurements of the activation energy for surface self-diffusion on Pt. Our calculation for Pt(100) gives a barrier of 0.97 eV, in very good agreement with the generalized-gradient approximation result of 1.04 eV.[26] As a further check, we calculate the barrier for the (111) Pt surface, obtaining a value of 0.26 eV compared to an experimental value of 0.25–0.26 eV,[27–29] and a value of 0.29–0.33 eV from other calculations.[30,31]

A list of all possible hops and the corresponding hop rates based on the atomic configuration on the surface is kept in memory in our simulation program; hop events are randomly chosen based on their probability and then executed, and then the list is updated to reflect the change in surface configuration. The clock, representing real time passed, is advanced by an amount proportional to the inverse of the sum of the rates of all the possible events.

A. Simulation results

A full simulation of growth was carried out at a variety of growth temperatures, from 325 to 1350 K, encompassing the temperature range in which anisotropy is observed experimentally in $CoPt_3$. Above 875 K the onset of bulk mobility is expected, which has been shown to destroy the metastable anisotropic state of codeposited $CoPt_3$;[4,5] since no interlayer exchange is permitted in this simulation, we do not expect to see this effect. Atoms are added at a constant flux, equivalent

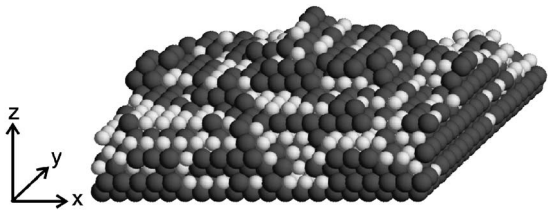

FIG. 2. Example output of simulation at 1350 K. Light gray balls are Co, dark gray are Pt. Growth is along the z axis; periodic boundary conditions are applied at the edges in the xy plane. The topmost layers are incomplete, while the lower layers are completely filled. Note the planar clusters of Co visible at the surface.

to 0.2 monolayers/second, randomly choosing cobalt or platinum with a weighted probability to give the correct composition. This rate is chosen to be comparable to the deposition rate in earlier investigations of e-beam deposited samples.[4,5] Between adatom events many hopping events occur, leading to surface rearrangement according to the same rules as in the single-layer simulation. Depositions were simulated in 20×20 and 50×50 arrays of atoms with periodic boundary conditions, such that atoms hopping to the right at the right edge will appear on the left edge, similar for the top and bottom edges. In order to ensure that the results were not dependent on the initial conditions, three deposition simulations were carried out at each temperature, with a different random underlayer each time.

In post-growth analysis, we look only at layers that are completely filled with atoms in the resulting simulated films. Film growth was typically simulated to a thickness of greater than 20 monolayers, giving good statistics for the fully buried layers and allowing us to observe whether the structure is stable or whether it varies with film thickness. As an example, a graphical representation of the result of a simulation at 1350 K is shown in Fig. 2, after the deposition of several monolayers. It is in the topmost, incomplete layers that atoms are free to move during the simulation. We note the planar clusters of Co are that are visible at the surface in this figure.

We define α as the fraction of the four in-plane NN sites occupied by Co, and β as the fraction of the eight out-of-plane NN sites occupied by Co, so that $(\alpha-\beta)$ is a measure of the structural anisotropy. Note that $(\alpha-\beta)$ would reach unity in a perfectly layered film. We plot $(\alpha-\beta)$ in Fig. 3, showing that anisotropy unambiguously develops with increasing deposition temperatures, exactly as seen in experiments. While only the difference is plotted, we note that in the simulation at 675 K the in-plane fraction is enhanced to 0.273 while the out-of-plane fraction is reduced to 0.221, compared to a random-mixture value of 0.25 for both. The 20×20 data show more scatter than the 50×50 atom simulations, but since they show the same trend with temperature (despite the large size difference), we conclude that the effect is not strongly dependent on the size of the simulated system. The self-consistency between the 20×20 and 50×50 results is the only test we have to show that this is a large enough system to adequately describe the process.

One additional simulation was carried out at an extremely high temperature of 1350 K. The results clearly demonstrate

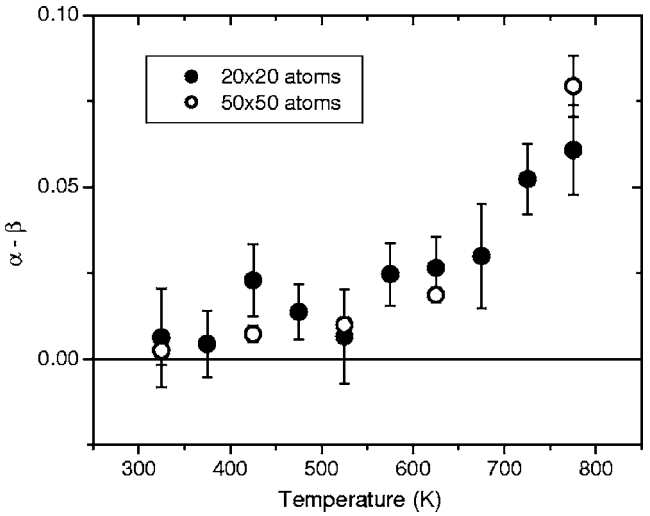

FIG. 3. Anisotropy $(\alpha-\beta)$ for simulated depositions as a function of temperature. Error bars represent variations between repeated simulations with different, random seeds. Note that the positive trend with increasing temperature continues out to a temperature of 1350 K (not plotted), for which $(\alpha-\beta)=0.26$.

the effects expected from the energetics, with Co segregated to step edges on the surface. The resulting anisotropy is high, with $\alpha=0.45\pm0.01$, $\beta=0.19\pm0.01$, giving $(\alpha-\beta)_{1350\ \mathrm{K}}=0.26$. Clusters of Co are clearly visible at the edges on the surface in the picture of the simulation results for this temperature, shown in Fig. 2

A strong indication of the correlation between anisotropy and Co edge fraction in these simulations is given in Fig. 4, in which we plot the fraction of surface edge sites occupied by Co atoms (at the top incomplete layer of the completed films). The expected value for a completely random film is 0.25, as noted by the horizontal dashed line on the plot.

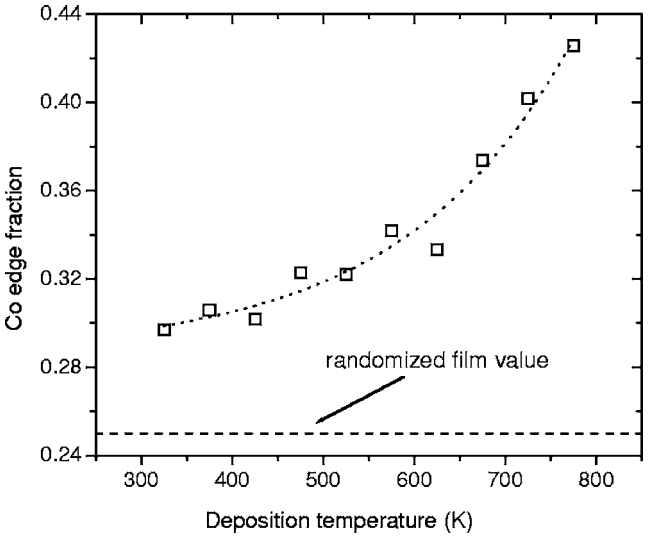

FIG. 4. Co edge-occupation fraction for the top surface of the completed films versus deposition temperature, for a series of 20×20 runs. The dashed line at 0.25 represents the value expected for a randomized film. The dotted line through the data is provided only as a guide to the eye.

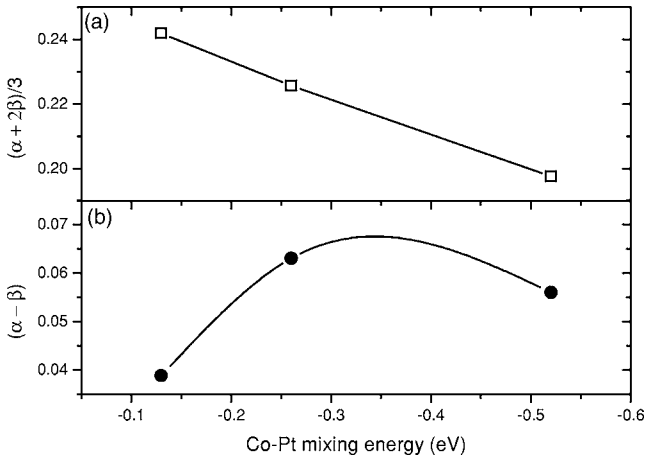

FIG. 5. Results of growth simulations at 775 K, varying the mixing energy: (a) the average number of Co NN per Co atom $(\alpha+2\beta)/3$, and (b) the anisotropy $(\alpha-\beta)$. The lines through the data are provided only as guides to the eye.

There is clearly a large enhancement in the Co edge occupation, and the temperature dependence of this enhancement is very similar to that seen in the anisotropy in Fig. 3, with a sharp increase at higher temperatures and a leveling off near room temperature. We suggest that growth conditions which favor a more fractal surface with more step edges, and favor Co edge segregation also lead to high anisotropy.

The mixing energy we used is $E_{\text{mixing}}=-0.26$ eV, appropriate for a small amount of Co dissolved in Pt;[16] a slightly less-negative E_{mixing} is expected for larger amounts of Co, when Co-Co interactions are no longer negligible. The growth simulation was repeated with different mixing energies for Co and Pt in order to isolate this contribution to the total energy and its effect on growth dynamics, clustering, and anisotropy. The value of $(\alpha+2\beta)/3$ is the average fraction of Co NN for each Co atom, which would reach unity for a completely three-dimensionally clustered material, zero for a material with perfect short-range order (in which each Co is completely surrounded by Pt), and 0.25 for a random mixture of 1 Co: 3 Pt. This value, which is a measure of the short-range order in the simulated films, is plotted in Fig. 5(a) along with the chemical anisotropy $(\alpha-\beta)$ in Fig. 5(b). We see a linear decrease in $(\alpha+2\beta)/3$ with increasingly negative mixing energy; the intercept of 0.25 for zero mixing energy is intuitive as a random mixture is favored in this case, while the system heads toward perfect short-range order (no Co-Co NN: $\alpha=\beta=0$) with more negative mixing energy. Earlier studies also predict this trend in the short-range order as a function of mixing energy.[32] By contrast, in the $(\alpha-\beta)$ data we observe a peak at the experimental value of $E_{\text{mixing}}=-0.26$ eV. This suggests that the proposed mechanism of anisotropic growth is strongest in materials with a specific mixing energy, and that Co and Pt have a mixing energy which may be nearly optimal for this growth effect. This agrees well with our earlier contention that the details of the energetics at the surface are responsible for segregation and thus anisotropy, as changing the energy balance in either direction leads to a reduction in the anisotropy in the simulated films.

In the analysis of the final simulated films, we found no thickness dependence to the observed anisotropy; the amount of clustering did not change with the addition of additional layers, and there was no systematic increase or decrease with layer number. This is consistent with experimental observations. The number plotted in Fig. 3 is the average of the value for all complete layers.

IV. DISCUSSION AND CONCLUSIONS

In the simulated growth of $CoPt_3$, we see that the edge segregation of Co increases with increasing temperature. We are below the temperature regime where random thermal motion would drive the system back toward randomness, as increasing temperature gives a monotonic increase in segregation.

The simulations show development of a clear structural anisotropy with increasing growth temperature, consistent with the Co NN anisotropy observed via EXAFS analysis in real codeposited films[6–8] and with the resulting observed magnetic anisotropy. When we compare $\alpha_{\text{sim}}(675\text{ K})=0.273$ with $\alpha_{\text{experiment}}(673\text{ K})\sim 0.5$ and $\beta_{\text{sim}}(675\text{ K})=0.221$ with $\beta_{\text{experiment}}(673\text{ K})=0.16$, we see that the anisotropy in the simulated films is smaller than that observed in real films. This is likely due to the exclusion in this model of more complicated surface kinetic processes such as interlayer transport, near-surface coordinated exchange processes, longer range hops, and other surface diffusion processes which enhance the probability of Co step edge segregation (but without altering the basic energetic idea of Co step edge segregation leading to anisotropy). Simulations at 1350 K produce values for α and β which are comparable to the experimental values for films grown at 673 K, showing that it is possible to achieve high anisotropy within the framework of our model if surface diffusion is high. We note that the lowest temperature at which the anisotropy first appears in our simulations is close to the experimentally observed value for the magnetic anisotropy of around 475 K, and the thickness-independent structural anisotropy in the simulated films is consistent with experimental results for the magnetic anisotropy of codeposited $CoPt_3$ films.[5]

Experimental work in our laboratory has shown a strong correlation between the density of steps found on the film surface and the magnetic anisotropy of the film.[13] In this work, films were prepared with differing amounts of surface roughness through the addition of a surfactant during the growth (oxygen), and the strength of the anisotropy was found to vary inversely with the roughness, and was quantitatively correlated with high step densities observed in atomic force microscope images of the surface. This further supports the contention that surface step edges are critical in the formation of the anisotropy.

The results of this paper are not limited to magnetic systems where the anisotropy is easily observed. We suggest that step-edge segregation resulting in clustering and anisotropic pair coordination is an important and not-yet appreciated effect in all multicomponent materials growing by island growth processes. We predict that the strongest structural anisotropy will occur when there is a negative en-

ergy of mixing together with a segregation energy which changes sign according to the coordination number, as is the case with Co-Pt mixtures.

In conclusion, we find from calculations using the TB-SMA potential that Co segregates to the edges of surface steps in Co-Pt alloy films. Kinetic Monte Carlo simulations of film growth, with hopping probabilities determined by this potential, clearly show structural anisotropy with an enhancement in Co-Co bonding in plane and a simultaneous reduction in Co-Co bonds out of plane. This agrees with EXAFS data for $CoPt_3$ codeposited films, in which the perpendicular magnetic anisotropy has been attributed to growth-induced Co clustering. To the best of our knowledge, this is the first microscopic explanation offered to date for the presence of growth temperature induced Co clustering for Co-Pt alloys which does not rely on a particular growth direction. Control of island growth and step-edge density thus offers a means for controlling the clustering with is necessary for the formation of perpendicular magnetic anisotropy in Co-Pt alloy films.

ACKNOWLEDGMENTS

Work supported by DOE Grants No. DE-FG02-04ER46100 and No. DE-AC03-76SF00098. The authors would also like to thank Christian Ratsch and Yana Landa for valuable discussions

*Currently at Metallurgy Division, National Institute of Standards and Technology, Gaithersburg, Maryland. Electronic address: bbm@nist.gov

†Physics Department, University of California at Berkeley; Materials Sciences Division, LBNL, Berkeley, California.

[1] C. J. Lin and G. L. Gorman, Appl. Phys. Lett. **61**, 1600 (1992).

[2] D. Weller, H. Brandle, G. Gorman, C. J. Lin, and H. Notarys, Appl. Phys. Lett. **61**, 2726 (1992).

[3] D. Weller, H. Brandle, and C. Chappert, J. Magn. Magn. Mater. **121**, 452 (1993).

[4] P. W. Rooney, A. L. Shapiro, M. Q. Tran, and F. Hellman, Phys. Rev. Lett. **75**, 1843 (1995).

[5] A. L. Shapiro, P. W. Rooney, M. Q. Tran, F. Hellman, K. M. Ring, K. L. Kavanagh, B. Rellinghaus, and D. Weller, Phys. Rev. B **60**, R12826 (1999).

[6] J. O. Cross, M. Newville, F. Hellman, B. B. Maranville, Y. U. Idzerda, S. Stadler, and V. G. Harris (unpublished).

[7] C. Meneghini, M. Maret, V. Parasote, M. C. Cadeville, J. L. Hazemann, R. Cortes, and S. Colonna, Eur. Phys. J. B **7**, 347 (1999).

[8] T. A. Tyson, S. D. Conradson, R. F. C. Farrow, and B. A. Jones, Phys. Rev. B **54**, R3702 (1996).

[9] Y. Gauthier, R. Baudoing-Savois, J. M. Bugnard, U. Bardi, and A. Atrei, Surf. Sci. **276**, 1 (1992).

[10] M. De Santis, R. Baudoing-Savois, P. Dolle, and M. C. Saint-Lager, Phys. Rev. B **66**, 085412 (2002).

[11] J. M. Bugnard, R. Baudoing-Savois, Y. Gauthier, and E. K. Hill, Surf. Sci. **281**, 62 (1993).

[12] C. Kittel, *Introduction to Solid State Physics*, 6th ed. (Wiley, New York, 1986).

[13] B. B. Maranville, Ph.D. thesis, Chap. 6.

[14] F. Cleri and V. Rosato, Phys. Rev. B **48**, 22 (1993).

[15] The energy prefactors A, ξ used in our paper are exactly a factor of 2 higher than in Ref. 14. The discrepancy is perhaps simply a definition problem, but using their values to fit the total bond energy per atom to the cohesive energy of the solid per atom we suggest is double counting, and results in the cohesive energy being twice its actual value.

[16] A. R. Miedema, P. F. de Chatel, and F. R. de Boer, Physica B & C **100**, 1 (1980).

[17] M. Hansen and K. Anderko, in *Constitution of Binary Alloys* (McGraw-Hill, New York, 1985), p. 492.

[18] A. V. Ruban, H. L. Skriver, and J. K. Nørskov, Phys. Rev. B **59**, 15990 (1999).

[19] P. Gambardella, M. Blanc, L. Bürgi, K. Kuhnke, and K. Kern, Surf. Sci. **449**, 93 (2000).

[20] P. Gambardella and K. Kern, Surf. Sci. **475**, L229 (2001).

[21] J. Jacobsen, K. W. Jacobsen, P. Stoltze, and J. K. Norskov, Phys. Rev. Lett. **74**, 2295 (1995).

[22] M. O. Pedersen, L. Osterlund, J. J. Mortensen, M. Mavrikakis, L. B. Hansen, I. Stensgaard, E. Laegsgaard, J. K. Norskov, and F. Besenbacher, Phys. Rev. Lett. **84**, 4898 (2000).

[23] M. Bott, M. Hohage, M. Morgenstern, T. Michely, and G. Comsa, Phys. Rev. Lett. **76**, 1304 (1996).

[24] J. Ellis and J. P. Toennies, Phys. Rev. Lett. **70**, 2118 (1993).

[25] A. Ulitsky and R. Elber, J. Chem. Phys. **92**, 1510 (1990).

[26] P. J. Feibelman and R. Stumpf, Phys. Rev. B **59**, 5892 (1999).

[27] M. Bott, M. Hohage, M. Morgenstern, T. Michely, and G. Comsa, Phys. Rev. Lett. **76**, 1304 (1996).

[28] P. J. Feibelman, J. S. Nelson, and G. L. Kellogg, Phys. Rev. B **49**, 10548 (1994).

[29] K. Kyuno, A. Golzhauser, and G. Ehrlich, Surf. Sci. **397**, 191 (1998).

[30] G. Boisvert, L. J. Lewis, and M. Scheffler, Phys. Rev. B **57**, 1881 (1998).

[31] P. J. Feibelman, Phys. Rev. Lett. **81**, 168 (1998).

[32] P. W. Rooney and F. Hellman, Phys. Rev. B **48**, 3079 (1993).